Insulating behavior of metakaolin-based geopolymer materials assess with heat flux meter and laser flash techniques

E. Kamseu · B. Ceron · H. Tobias · E. Leonelli · M. C. Bignozzi · A. Muscio · A. Libbra

Abstract Thermo physical behavior of metakaolin-based geopolymer materials was investigated. Five compositions of geopolymers were prepared with Si/Al from 1.23 to 2.42 using mix of sodium and potassium hydroxide ($\sim$7.5 M) as well as sodium silicate as activator. The products obtained were characterized after complete curing to constant weight at room temperature. The thermal diffusivity (2.5–4.5 $\times$ 10^{-7} m^2/s) and thermal conductivity (0.30–0.59 W/m K) were compared to that of existing insulating structural materials. The correlation between the thermal conductivity and parameters as porosity, pore size distribution, matrix strengthening, and microstructure was complex to define. However, the structure of the geopolymer matrix, typical porous amorphous network force conduction heat flux to travel through very tortuous routes consisting of a multiple of neighboring polysialate particles.

Introduction

Insulating materials are using to slow heat transfer. In the modern times, as mankind became more sophisticated, a wide range of largely synthetic materials are developed which proves to be far superior insulators. However, with each step away from the natural substances, mankind not only saw incremental improvements in the ability to insulate, but also huge increases in the environmental and health problems caused by various synthetic insulation materials.

More sustainable insulating matrices have been developed from alumina (Al$_2$O$_3$) and silica (SiO$_2$) or combination of both. Two oxides with thermal conductivity of 6–10 and 18–30 W/m K, respectively for SiO$_2$ and Al$_2$O$_3$ in crystalline form. The transformation of the crystalline structure to amorphous creates a high level disorder in the special arrangement of atoms and decreases the thermal conductivity to $\sim$1.5 W/m K. Additional voids and pores will enable the amorphous structure to be filled in air and insulating gas with consequence in further decrease of heat transfer ability through the amorphous matrix.

The gas-filled pores have a small role to play, the solid matter structures a decisive one. The structure includes the bulk matter and the voids (pores). The chemical composition of the material will determine the thermal conductivity while the pores content will affect the effective value. Thus, the insulating behavior of a material is governed by parameter such as porosity, gas- and liquid-filled pores, mineral content, and grain size distribution [1–5]. Hence, insulating materials can be produced by various combinations of

E. Kamseu (✉) · E. Leonelli
Department of Materials and Environmental Engineering, University of Modena and Reggio Emilia, Via Vignolese 905/A, 41125 Modena, Italy
e-mail: kamseuelie2001@yahoo.fr; elie.kamseu@unimore.it

B. Ceron · H. Tobias
Department Werkstoffwissenschaften Lehrstuhl fur Glas Und Keramik, Universtat Erlangen-Nurnberg, Martensstr. 5, 91058 Erlangen, Germany

M. C. Bignozzi
Department of Civil, Environmental and Materials Engineering, University of Bologna, Via Terracini 28, 40131 Bologna, Italy

A. Muscio · A. Libbra
Department of Mechanical and Civil Engineering, University of Modena and Reggio Emilia, Via Vignolese 905/B, 41125 Modena, Italy

materials and microstructures to achieve desired thermal comfort with reduced energy consumption. Both reflective and mass insulation involve placing a solid material between the warm and the cool regions to reduce heat flow across the insulation region.

Amorphous alumina is prepared by various methods for applications in the area of electronics. Al_2O_3 thin films form dielectric layers which are applied as electrical insulating substrates in multilayer technologies [6].

Amorphous nature of silica is generally exploited for insulating applications. Amorphous silica causes a decrease in the thermal conductivity and even electrical resistivity [7, 8]. Some of the most diffused porous aluminosilicates has been developed through sintering route at high temperature with very high energy consumption. When clayey materials are subjected to thermal treatment at temperature between 500 and 800 °C [9, 10], they transform into amorphous phase or mixture of amorphous and crystalline phases. This transformation contributes to reduce the thermal diffusivity and thermal conductivity of the matrix enables elaboration of potential insulating materials.

An environmentally friendly solution to develop porous amorphous insulating matrices is geopolymerization of amorphous aluminosilicates. Insulating geopolymer should have advantages of being much safer than most of the insulation materials described in the literature, and more environment friendly, since they are essentially comprised of the same components as the earth with low energy required for processing. It would be a significant improvement over the prior art to provide insulation materials and methods for their manufacture more environmentally neutral with production cost equal or even lower than currently used insulation materials. Further, it would be significant advancement in the art to provide insulation matrix which can be rapidly formed while maintaining their shape, materials which are not only light-weight but have structural support and is completely non flammable. The insulation matrix within the scope of this study is particularly useful in most applications or areas where insulating materials are now used. They are particularly useful in the construction industry because of their low cost and light-weight, in insulating building walls and for covering heating and cooling ducts therein, as well as with many types of refrigeration equipment.

A geopolymer is an inorganic aluminosilicate, synthesized from predominantly silicon and aluminum materials of geological origin, or by-products such as coal fly-ash and granulated blast furnace slag [11]. Geopolymers are chemically designed as polysialates matrices. The polysialates network, chain, and ring of polymers consist of SiO_4 and AlO_4-tetrahedra linked in an alternating sequence by sharing all of the interstitial oxygens. Positive ions (Na^+, K^+, Li^+, Ca^{2+}, …) must be present in the framework

cavities to balance the negative charge of Al^{3+} in four fold coordination. Polysialate has the empirical formula: $Mn[(SiO_2)z \cdot AlO_2]n \cdot wH_2O$, where M is a cation, usually an alkali, n is a degree of polycondensation, $w \leq 3$ and z is 1, 2, or 3 [12].

In a microstructural point of view Geopolymer materials consist of nanoparticulates ranging from 5 to 15 nm in dimensions separated by nanoporosity whose features are the other of 3–10 nm. A nanoporous, sponge-like microstructure characteristic of a fully reacted region of polysialates. The size of pores formed in these materials has been observed to be so small as to be effectively part of the skeletal framework, which reduces the effective density of the gel and reduces the accessible pore volume. Therefore, the distribution and interconnectivity of the pore structure, the short-range ordering of the gel phase, and the nominal composition are all likely to play roles in determining the thermophysical transport properties of geopolymer network [13]. By using the appropriate alkali concentration to activate and consolidate amorphous aluminosilicate, a porous matrix can be obtained with relatively low alkali ions while maintaining high strength, light-weight, and sponge-like structure. During geopolymer process, significant amount of entrained air can be added to the structure. Carbone dioxide (CO_2) will react with alkali ions in solution to increase both the gas concentration in the structure.

The topic of this study is focused on the thermo physical characterization of geopolymers obtained from thermally treated clayey materials. The thermal conductivity of geopolymer available in the literature concern structural matrices [13] and geopolymer foams [14, 15] in which high concentration of alkali used to dissolved silica and enhance the reactivity evidences the problem in the effectiveness of the insulating ability of the respective matrices. Moreover, in building application, the challenge is that of having good insulating structure with optimum mechanical strength and stability under environmental stresses. This still a goal since we know the geopolymer develop with inappropriate Si/Al molar ratio and alkali ions content are generally non stable under leaching stresses or when cycles of heating and cooling have to be considered. Hence this paper present the thermo physical properties of geopolymers with various Si/Al previously studied for their polycondensation, mechanical properties and short-term durability under environmental stresses.

Materials and experimental procedures

Materials and geopolymers preparation

One standard and one sand-rich kaolinitic clays (MI-PROMALO, Cameroon) were used in this study. The two

materials were calcined at 700 °C for 6 h to obtain anhydrous aluminosilicates identified as Al-rich (51.59 wt% of Al_2O_3) metakaolin (MK-M) for the standard and Si-rich (70.11 wt% of SiO_2) metakaolin (MK-T) for sand-rich. MK-M has 39.34 wt% of SiO_2 and 5.11 wt% of TiO_2 while MK-T has 28.21 wt% of Al_2O_3 and 0.66 wt% of TiO_2. The others elements were <3 wt% for MK-M and <2 wt% for MK-T. MK-M was amorphous at XRD while MK-T patterns present intensive peaks of quartz.

Five mixes were prepared from the two calcined with respective Si/Al molar ratios of 1.15, 1.40, 1.59, 1.86, and 2.19, respectively. Mixture of sodium hydroxide, potassium hydroxide, and sodium silicate were prepared with the volume ratio 1:1:2 and used as alkaline solution. The sodium and potassium hydroxide solutions were prepared by dissolving respective pellets (99.6 wt%, Carlos Erba, Italy) in the distilled water to have 7.5 M. The sodium silicate solution was a viscous liquid from Ingessil (Italy) with $SiO_2/Na_2O = 3$, density of 1.38 g/cm^3, and the L.O.I of 60 wt%.

Each of the five mixes of metakaolin powders was ground to fine particles (<80 μm), dissolved in alkaline solution with the solid/liquid ratio of 1.66 g/mL (water to geopolymer proportion of 0.38). The alkaline solution is stirred for 5 min before the addition of powder. The viscous pastes obtained were ball milled for another 5 min and poured in the Teflon molds. Specimens M, 75M, TM, 25M, and T were obtained for the respective above amorphous aluminosilicate compositions. The NaK/Al ratios were 0.83, 0.89, 0.96, 1.05, and 1.16, respectively, while the final Si/Al ratios were 1.23, 1.55, 1.79, 2.07, and 2.42 in the final geopolymer pastes. The design of the compositions of this study has been developed first by primary constraints of the structural nature and strength and by seeking the subset of materials which maximize the performance of the components for a successful product. With respect to an insulation barrier, those primary constraints include minimal weight, maximum strength and toughness requirements. In this application where insulation and not strength is the overriding factor, manual or mechanical vibration of the pastes generally used to remove pores and air in geopolymer pastes was avoided with the aim to improve the incorporation of air and gas into the final geopolymer matrices.

Appropriates shapes were prepared for different methods of thermal conductivity measurement used. For Laser Flash method, disks of 10 mm of diameter with 1.8 mm thickness were prepared.

The specimens were directly sealed from atmosphere for 72 h, then curing continuous at ambient (21 ± 1 °C and 54% of relative humidity) temperature for at least 28 days before characterization.

Characterization of geopolymer materials

Mineral phase content

The X-ray patterns were acquired using an X-ray powder diffractometer (XRD), CuKα, Ni-filtered radiation (the wavelength was 0.154184 nm), Phillips Model PW3710. The radiation was generated at 40 mA and 40 kV. The analysis was performed in fine grains of ground geopolymers, pieces obtained after compressive strength testing. Specimens were step-scanned as random powder mounts from 5 to 70° 2θ at 0.05 2θ steps and integrated at the rate of 2 s per step. Crystalline phases were identified by comparison with PDF standards (Powder Diffraction files) from ICDD.

Porosity

A Mercury intrusion type mercury intrusion porosimeter (MIP), Carlo Erba 2000 equipped with a macropore unit, Model 120, Fison Instrument was used. Geopolymer specimens were crushed to particle size range of approximately 8–10 mm (total volume ∼ 1 cm^3). The specimens used for the measurements were obtained from fractured pieces of mechanical tests. The analysis was performed with a 2,000 bar maximum injection pressure for pore size in the range between 0.004 and 10 μm. Pore size distribution from mercury intrusion data was calculated by Washburn Eq. 1, assuming a contact angle of 141.3° and a Hg surface tension of 480 dyn/cm.

$$r = -\frac{2\gamma \cos\theta}{p} \qquad (1)$$

where r is the radius of the pore or pore entrance just intruded by mercury, which has a surface tension γ and a contact angle θ with the material tested, under pressure p.

The primary data of pressure, intruded mercury volume, sample mass, and sample volume (pycnometrically determined by mercury) are the basis to calculate the pore size distribution, the cumulative pore volume at maximum or defined pressure, characteristics such as average pore radius or median pore radius, the bulk density, the apparent density are also evaluated.

The microtomograph measurements

The SkyScan microtomograph is a compact desktop X-ray tomography system with microscopic resolution. Microtomography works in exactly the same way as the X-ray tomography systems (CAT-scans) used in medicine but with much finer resolution. Internal structures are reconstructed as a set of flat cross sections which are then used to analyze the two and three dimensional morphological

parameters of the object. The process is nondestructive and requires no special preparation of the specimen. The 3D spatial resolution of the SkyScan desktop microtomograph is 5 μm and features as small as 1 μm can be visualized.

The μCT measurements were done using a Skyscan 1172, Skyscan B.V., Leuven, Belgium at 80 kV with 100 μA, no additional filtering and a image pixel size of 10.1 μm. Cell and strut size evaluation were done with CT-Analyzer (CTan), 1.10.0, Skyscan B.V., Leuven, Belgium on a minimum of 250 slices of each sample. Visualization of the scanned images was done using Amira 5.3.2, Visage Imaging GmbH, Berlin, Germany with Voltex displaying mode. Scanning and reconstruction time was each 90 min per specimen on a quad core E9500 PC with 8 GB RAM. The 3D evaluation took between 1 and 4 h per specimen depending on the porosity rate with a total amount of 60 GB data.

Thermal conductivity

Thermal conductivity laser flash method

The specimens prepared were controlled to being homogeneous enough without fissures and holes. The surface was then coated with gold and carbon. Gold was deposed on the surface to retard thermal contact into semi-transparent material. Surface treatment was completed by carbon powder spray on the surface to efficiently absorb the laser beam. The measurements were performed in vacuum below 3×10^{-3} Pa. The method consists of illumining the front face of the disk with a short laser pulse, creating at the surface a heat pulse when the light is absorbed. The Laser used was a QUANTEL type with wavelength of 1053 nm with a maximum energy of 100 mJ. The duration of pulse was 350 μs. The thermal diffusivity, α, is deduced from the thermal transient of the rear face, called thermogram. The temperature rise at the rear surface was measured by an In–Sb infrared detector, after the front surface of the specimen was heated by the ruby laser pulse. The data were collected and analyzed by an Oscilloscope type TEKTRONIX TDS3012. The thermal conductivity λ is then calculated as:

$$\lambda = \rho \cdot C_p \cdot \alpha \tag{2}$$

where ρ is the density, C_p is the heat capacity determined by DSC method [16], and α is the thermal diffusivity.

Thermal conductivity by heat flux meter method 1

The heat flux meter (ASTM C518, ISO8301) uses homogeneous samples with good planarity. The procedure is based on multi thicknesses of the specimen. Thermal contact (or contact resistivity) may cause huge errors of thermal conductivity measurements if it is not taken into account. Specimen's thermal resistance is equal to the sample's thickness x (m) divided by its thermal conductivity λ (m^2K/W).

$$R_{\text{sample}} = x/\lambda \tag{3}$$

Thermal contact resistance (R_{contact}) depends on the materials, their roughness, and the interface pressure and is equal to temperature difference between the two contacting surfaces δT divided by heat flux q (W/m^2).

$$R_{\text{contact}} = \delta T/q \tag{4}$$

The thermal resistance of the specimen placed into the instrument is equals to:

$$R_{\text{total}} = x/\lambda + 2R_{\text{contact}} \tag{5}$$

The total resistance is proportional of the heat flux q across the specimen which is function of the temperature difference ΔT between instrument's plates and inversely proportional to the total resistance R_{total} (W/m^2):

$$q = SQ = \Delta T/R_{\text{total}} = \Delta T(x/\lambda + 2R_{\text{contact}}) \tag{6}$$

In case of thermal insulation materials (small λ) the specimen's thermal resistance is large and thermal contact resistance can be neglected. Plotting the graph of the thermal resistance as function of thickness, extrapolation down to zero thickness gives the value of thermal contact resistance of the two surfaces ($2R_{\text{contact}}$). Reciprocal of the slope ($\Delta x/\Delta R_{\text{total}}$) is equal to the correct thermal conductivity of material:

$$\lambda = (x_2 - x_1)/(x_2/\lambda + 2R_{\text{contact}} - x_1/\lambda - 2R_{\text{contact}}) \tag{7}$$

where x_1 and x_2 are thickness of the thin and thick specimens. Multi-thickness gives better accuracy. Thermal contact resistances are assumed to be the same for all the material specimens. So the specimen's surface finish should have the same quality. For this study, we used quadratic specimens 30×30 mm^2 with various thicknesses from 1.5 to 6 mm. The flow meter used was of the following model.

Heat flux meter method 2

The thermal conductivity of the porous bodies was measured on disk specimens of a diameter 18.85 mm and thickness ranging between 0.6 and 2.8 mm using a reference body made of brass in a self-made apparatus constructed accordingly to DIN51908. A calibration curve relating the thermoelectric power U with the thermal conductivity and fitting the data to the Eq. 8 by the least squares method. From the calibration curve, constants a and b were computed (1.89 and 2.68, respectively) and with them the thermal conductivity of porous specimens was determined as:

$$U = \frac{a}{b/(\lambda/l) + 1} \qquad (8)$$

where λ is the thermal conductivity of the specimen and l is its thickness.

Water charging and decharging capacity of geopolymer materials

Exposition at ambient temperature and weight loss at temperatures between 20 and 100 °C was used to investigate the capacity of the materials to accumulate and lose humidity in relation to their mechanical stability. The specimens were first cured up to constant weight in laboratory (20 ± 5 °C and 55% of relative humidity). The specimens are placed in the oven at 100 °C for 24 h. The total weight loss is used to calculate the saturation in humidity (T) and the weight gained after oven (Tx) is measured progressively (in h). Tx/T is then calculated with time.

Results

Thermal diffusivity and thermal resistance

Volumetric heat capacity that characterizes the ability of geopolymer materials under study to adjust their temperature to that of surroundings is presented in Fig. 1. The thermal diffusivity determined using Parker's method is 2.25×10^{-7} m^2/s for sample M which has Si/Al molar ratio of 1.23. From XRD patterns (Fig. 2), it is possible to evidence the amorphous structure of the specimen with few small peaks of crystalline phase (α-quartz). With the increase of Si/Al, passing to the specimen 75M, the thermal diffusivity increases to 2.6×10^{-7} and 3.8×10^{-7} m^2/s; 3.85×10^{-7} and 3.8×10^{-7} m^2/s for MT, 25M, and T, respectively. This increase in thermal diffusivity is directly
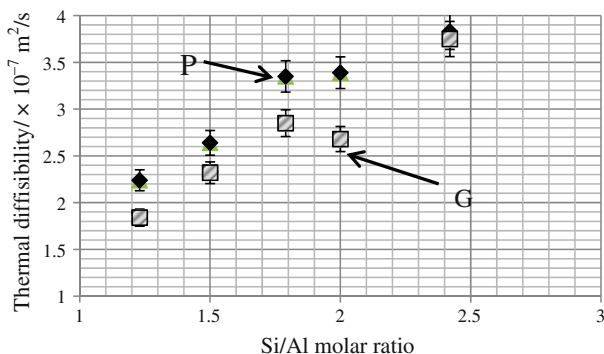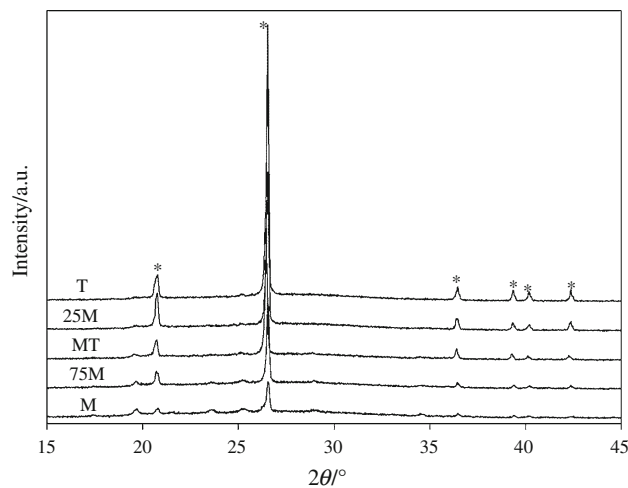

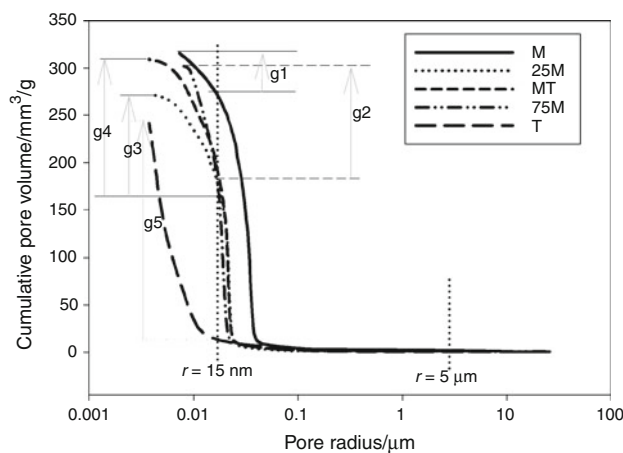**Fig. 2** XRD patterns of geopolymer compositions: *asterisk* quartz

Fig. 3 Pores size distribution in the Geopolymer compositions: g_1 (13.38), g_2(39.55), g_3(47.44), g_4(40.04), and g_5(93.63) represent the volume fraction (%) of gel pores of M, 75M, MT, 25M, and T, respectively

correlated to the increase of Si/Al as well as to the crystalline phase content (Fig. 2). As matter of fact, passing from M (Si/Al = 1.23) with major amorphous structure to 75M, MT, 25M, and T with 1.5, 1.79, 2.0, and 2.42 as respective value of Si/Al molar ratio, the XRD patterns indicate an increase in α-quartz content as it can be observed in Fig. 2; the amorphous structure presented by M moved to semi-crystalline as Si/Al molar increases.

The increase of the XRD peaks of α-quartz with Si/Al can be correlated with the variation in thermal diffusivity. Moreover, the increase in Si/Al contributes to a better polycondensation with the decrease of voids and pores size (Fig. 3), the density increases with the thermal diffusivity.

These results demonstrates that the thermal diffusion in geopolymers is fundamentally correlated to the composition, the mineral phases content and most important the

Fig. 1 Thermal diffusibility of geopolymer matrices as function of Si/Al molar ratio. *P* Parker, *G* Degiovanni 1/2

degree of crystallinity of the matrix. It should be noted that the increase of Si/Al molar ratio that have been described as important factor for the optimization of the geopolymer matrices with high strength is in contrast with the insulating behavior.

In the Fig. 4, the thermal resistance of each composition of geopolymers is plotted as function of the thickness. Under uniform conditions, the thermal resistance (R value) measures the ability of material to resist to heat transfer. The bigger the number, the better the building insulation's effectiveness. The geopolymer matrices behave like resistance in electrical circuits: increasing the thickness of the specimens (Fig. 4), the thermal resistance increases. During the thermal treatment of kaolin, the crystal orientations change and the thermal diffusivity decreases while the thermal resistance increases due to the transformation into amorphous structure. Benoit and Mainprice [17] demonstrated that both thermal diffusivity and anisotropy of quartz, second phase generally presents in kaolin, decrease with temperature up to 500 °C. The thermal diffusivity strongly decreases up to 572–574 °C, i.e., the α–β transition temperature. Hence both calcination of kaolin and transformation of residual quart participate to the development of disordered phases and relatively lowering thermal resistance. With the two heat flux meters, we observed

that the increase of the thermal resistance of the material with thickness. The thermal resistance of the specimen M and 75M (with low Si/Al ratio; low residual quartz content is above $6 \times 10^{-3} m^2/W\,K$ with specimens thickness of 2 mm. This value increases to $10 \times 10^{-3} m^2/W\,K$ for both specimens at 4 mm while at 6 mm, the thermal resistance is $14 \times 10^{-3} m^2/W\,K$ for M and $13 \times 10^{-3} m^2/W\,K$ for 75M. With the increase of Si/Al ratio, MT (1.79) presents a lower thermal resistance at high thickness ($<12 \times 10^{-3} m^2/W\,K$ at 6 mm). For specimens 25M and T, the tendency is for lower thermal resistance at low thickness compared to M and 75M (Fig. 4). The variation of the thermal resistance of geopolymers specimens follows that of the thermal diffusivity.

The linearity of this variation indicates that the two methods are indicated for the assessment of the geopolymer materials. The errors bars are indicative on the deviation from the two equipments.

Thermal conductivity

Measurements of the thermal conductivity of geopolymers specimens, following the described methods (laser flash and heat flux meter), were made. The results are presented in Fig. 5 where it can be observed the influence of the

Fig. 4 Variation of the thermal resistance R^* (m^2 K/W) with the thickness (m) of geopolymer materials
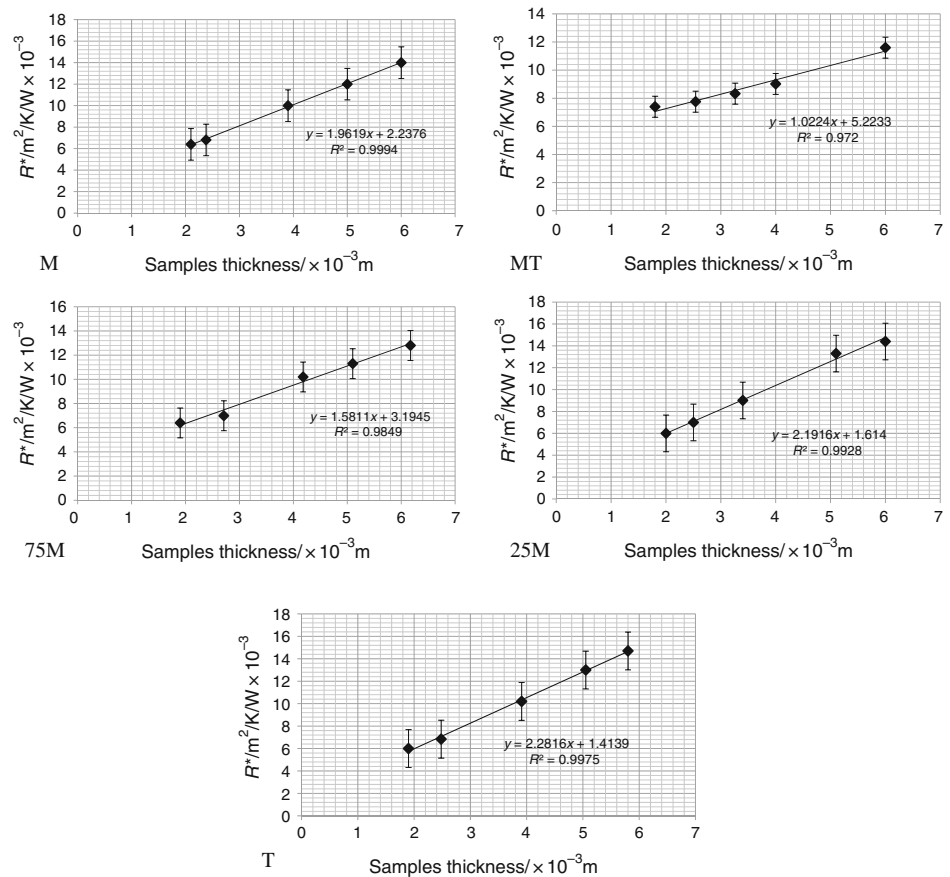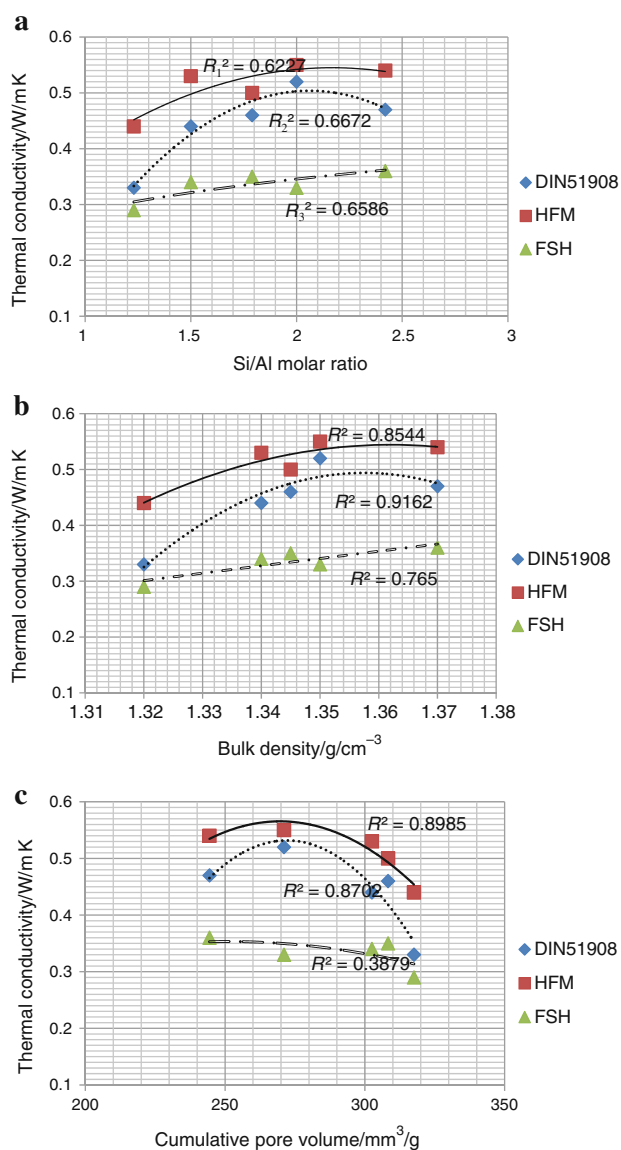
Fig. 5 Variation of the thermal conductivity (W/m K) with Si/Al molar ratio, bulk density and cumulative pore volume

density, the Si/Al ratio and that of the cumulative pore volume on the variation of the thermal conductivity. Laser Flash method (non-steady state) presents values of thermal conductivity relatively low with respect to the heat flux meter (steady state). The variation of the thermal conductivity with the Si/Al molar ratio was linear in the case of flash laser while in others cases a narrow variation were observed (Fig. 5a). The thermal conductivity of geopolymers varies between 0.30 and 0.59 W/m K with a standard deviation of 5% as indicated in the Fig. 5. The general trend is the increases of the thermal conductivity of the specimens of geopolymer materials with the increase of Si/Al molar ratio. This increase in thermal conductivity can be directly correlated with the variation of thermal diffusivity as described above.

The insulating ability of geopolymer materials is based on their porosity and the amorphous nature of their predominant phase [12, 13]. Literature described matrix of geopolymer as nanoporous, sponge-like microstructure characteristic of a fully reacted region of polysialates (Fig. 6). Hence, the matrix force the conduction of heat flux to travel through very tortuous routes consisting of a multiple of elementary thermal resistances located at the coalescences of neighboring polysialates particles. The difference in Si/Al molar ratio of the compositions of geopolymer materials under study consists in excess of Si that contribute to reinforce the polysialates formed (chains and rings of polysialates) or act as fillers for the good of the mechanical properties of the matrices (Table 1). Unfortunately, this supplement of Si that was found to be crystalline or semi-crystalline, residues of silica from the sand-rich aluminosilicate used do not contribute positively for the insulation behavior of the matrix of geopolymer. Consequence, the thermal conductivity increases with the increases of the Si/Al molar ratio as expected (Fig. 5b).

Considering the variation of the thermal conductivity of geopolymer materials with the cumulative pore volume, as reported in Fig. 5c, it can be observed that the thermal conductivity of geopolymer decreases with the increase of pores. The composition of geopolymer with the lower cumulative pore volume is the specimen T with 244.4 mm^3/g and 0.35 W/m K as thermal conductivity (Laser Flash Method). This value decrease to 0.32 and 0.28 W/m K, respectively for specimens 25M and M. Specimens with high cumulative pore volume (M and 75M) are characterized with additional macropores that affect the thermal conductivity and can potentially explain the linear correlation between the thermal conductivity (based on laser flash method) of the specimens with the cumulative pore volume. Similar situation was observed with the results of the thermal conductivity based on the DIN51908 norm (heat flux method 2). For the results, the correlation was linear with specimens with cumulative pore size higher than 250 mm^3/g and polynomial when all the specimens were considered. It should be noted that the values of thermal conductivity for heat flow meter 1 (HFM1) and HFM2 were closed, with deviation between them of about ±0.06, 0.47, and 0.53 W/m K, respectively for the specimen T and 25M for the cumulative pore volumes of 244 and 271.07 mm^3/g. The values of thermal conductivity of 0.53, 0.50, and 0.45 W/m K for MT (308.3 mm^3/g), 75M (302.5 mm^3/g), and M (317.55 mm^3/g) were obtained with HFM1. When consider the HFM2, these values become 0.45, 0.48, and 0.38 W/m K. The results for those specimens could have been affected by the relative heterogeneity of the specimens. Both series of values that correspond with the steady state measurement

of thermal conductivity differ from the series of values obtained with non-steady measurement (laser flash).

The above described results can be interpreted taking in consideration many sources of errors with origins related to the equipments and procedures. While the similitude of values between the two HFM is observed in Fig. 5b with specimens T, 25M and may be MT, the heterogeneity that characterizes others samples of geopolymers like 75M and M (due to the Si/Al ratio, the alkali content and pore size distribution) can justify the higher deviation observed within the results. Micrographs of Fig. 6 present geopolymer materials as typical non-crystalline materials. As we can observed from the matrix, M shows more fine grains resulting from the complete amorphous structure of calcined standard kaolin. By introducing silica-rich metakaolin, as from 75M, the microstructure is progressively transformed being coarse consistent with the formation of more larger grains of polysialates and higher silica residues from incomplete dissolution and polycondensation unlike dense and relative homogeneous matrix. From the MIP and microtomography (Figs. 3 and 7), it is observed that the low Si/Al (<2) remain with relative large pores (15 vol.% for M and 75M specimens). With Si/Al $\geq$ 2, the mean volume size of pores moves to low value and the volume of pores > 20 μm decreases less than 10 vol.% (Figs. 3 and 7). These variations of the porosity and pore size would have affected the thermo physical properties of the geopolymer specimens under studies.

Microstructure and humidity absorption in geopolymers

After the complete curing of geopolymers specimens up to constant weight, it was observed that M, 75M, and MT have 8.6, 8.4, and 8.1% of humidity in their respective matrices while values of 7.8 and 7.5% were recorded for 25M and T. Figure 8 presents the variation of ability of geopolymers compositions to absorb humidity with time (Tx/T). Tx is the percent of humidity absorb at the time t and T is the possible saturation. The ability to store the moisture and humidity up to the above described values is primarily linked to the amorphous nature, the porosity as well as the capacity of silica elements to fix water from air. From Fig. 8, it is observed that after drying at 100 °C, the rate of charging in humidity of samples is governed by the Si/Al molar ratio. The lower the Si/Al molar ratio the lower is the rate of humidity absorption. This behavior is in contrast with the cumulative pore volume and even with the pore size distribution. In fact, specimens 25M and T that present high rate of absorption have the lower cumulative pore volume (271 and 244 mm³/g for 25M and T, respectively) with the average pore size of 0.018 μm for 25M and 0.013 μm for T. For MT, 75M, and M, the cumulative pore volume is higher, 308, 303, and 318 mm³/g, respectively as the average pore size is 0.024, 0.025, and 0.031 μm (Fig. 3; Table 1). The volume fraction (%) of gel pores (pore size $\leq$ 15 nm) [8] are $X_1 = 13.4$ for M; $X_2 = 39.6$ for 75M; $X_3 = 47.4$ for MT; $X_4 = 40$ for 25M;

Fig. 6 Micrographs of geopolymer materials showing the amorphous nature of their structure with the grow of grains and coarsening structure as the Si/Al increase between 1.23 and 2.42
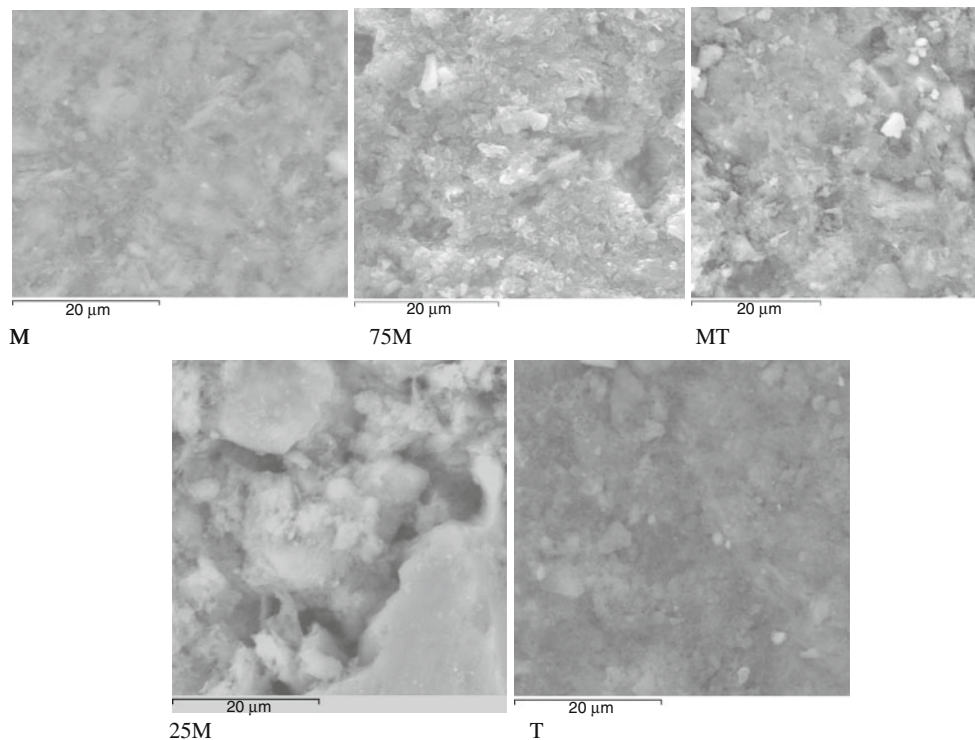
Table 1 Composition and physical characteristics of geopolymer materials

Samples	Si/Al	Na/Al	Bulk density/g/cm³	Cumulative pore volume/mm³/g	Average pore size/μm	Thermal capacity MJ/m³ K	Thermal diffusivity/10⁻⁷ m²/s
M	1.23	0.83	1.32	317.55	0.031	0.995	2.24
75M	1.50	0.89	1.34	302.50	0.026	1.015	2.64
MT	1.79	0.96	1.345	308.30	0.024	1.109	3.35
25M	2.00	1.05	1.35	271.07	0.018	1.112	3.39
T	2.42	1.16	1.37	244.42	0.013	1.109	3.83
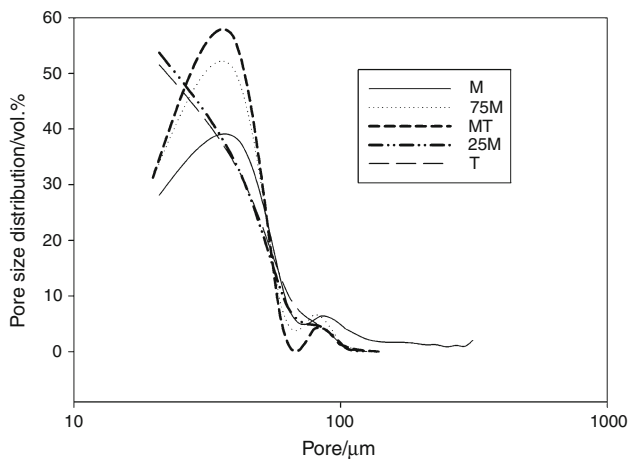
Fig. 7 Distribution of pores > 20 μm in geopolymer samples
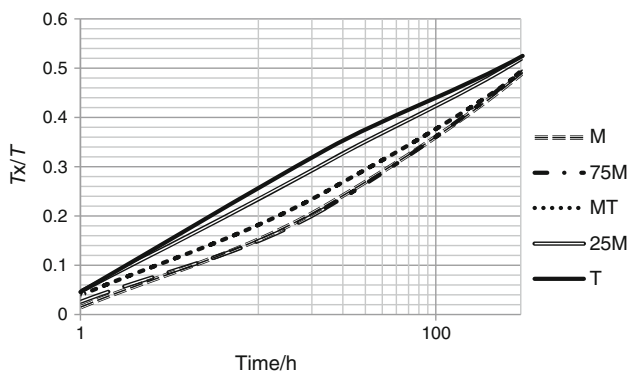
Fig. 8 Variation of the humidity absorbed by geopolymers compositions with time (h) in ambient atmosphere, Tx/T is the ratio of the percent of humidity at moment t and the total saturation

$X_5 = 93.6$ for T. The volume fraction of capillary pores ($r \geq 5$ μm) is very low for all the specimens. It is then suggested that during the charging in humidity of geopolymer specimens, two mechanisms take place:

(i) Chemical fixation of atmospheric water and air which is predominant and more important in the case of specimens with high Si/Al molar ratio.

(ii) Physical absorption of atmospheric water and air is the absorption by pores.

The fixation of atmospheric water by samples is interpreted with the chemical reaction of Si with OH^- to form $Si(OH)_4$. For specimens with low Si/Al molar ratio, it takes time for pores, micro cracks, and unreacted species to fix humidity since the active sites with silica are less numerous. This behavior of geopolymer materials can affect the variation of their thermal conductivity in service.

Discussion

The microstructure of metakaolin-based geopolymer materials and their thermophysical properties are primary linked to (i) the transformation of kaolin to metakaolin, (ii) the residual crystalline silica content of aluminosilicates precursors, as well as, (iii) the degree of polycondensation and structural reorganization of oligomers in polysialates including the pore development. This peculiarity tends to affect the final porosity and pore size distribution, two of the most important parameters of heat transfer in structural materials. The results of thermal diffusivity and thermal conductivity of our specimens instead of being interpreted as function of Si/Al only can be easily divided into two series: first series with M and 75M which we can be identified as Al-rich geopolymer and MT, 25M, and T series called Si-rich geopolymers. Figures 3, 4, and 5 demonstrated a real division between the two groups of materials.

The results obtained showed that geopolymer materials for structural applications developed thermal conductivity between 0.30 and 0.59 W/m K, demonstrating that low Si/Al (with fully amorphous structure as indicated in Fig. 6) with total porosity >40 vol% is compared with porous geomaterials developed with similar technology by Prud'Homme et al. [14, 15]. However, their thermal diffusivity of 5.9×10^{-7} m²/s is high compared to those obtained of Fig. 1 and can be explained by the relative high content of alkali used. Even though the authors obtained porous materials, the chemical composition contributes to affect the thermal transfer behavior in those specimens. Peter Duxson et al. [13] studied the thermal conductivity of metakaolin-based geopolymers and obtained value near to

0.8 W/m K. Even if the Na/Al was kept 1, the variation of silica content with sodium silicate tend to introduce more alkali in the matrix that finally affect the heat transfer behavior even in the situation of high porosity.

Apart from the composition design, accurate determination of thermal conductivity depends on the selection of test apparatus and experimental procedure. It is generally accepted that the most reliable values of λ are obtained by measuring in steady state conditions (transient methods allow somewhat faster measurement). The steady state techniques most commonly used for commercial λ-value measurement are the HFM method; the guarded hot-plate method, an absolute technique [18].

The specific error sources are temperature variation and non-linear heat flow (a progressive drift in the overall temperature or a fluctuation across the platen surface). Edge losses resulting from the non-linear heat flow would still be considered a major source of error even though the normalizing effect of the calibration makes edge losses less important for HFM instruments. Sources of errors are also associated as far as steady state methods are concerned, with Q/A (heat flux), Δx, and ΔT.

The original laser pulse method of measuring thermal diffusivity proposed by Parker et al. [19]. assumes ideal boundary and initial conditions, i.e., zero heat loss, infinitely short pulse, and uniform heating of the sample face. Thanks to the theoretical works of many researchers, the original concept has been gradually improved to account for real experimental conditions [20–22].

Conclusions

The paper assesses the heat transfer through metakaolin geopolymer matrices. Results of our investigations indicated that:

- Thermal diffusivity, thermal resistance, and thermal conductivity of geopolymer materials are associated to the porosity and pore interconnectivity that characterizes this type of materials.
- Both composition and porosity (cumulative pore volume and pore size distribution) are main important factors affecting the heat flow in the geopolymer matrices.
- The method of measurement of thermal conductivity of geopolymer can influence the final results mainly due to some deviation associated to the experimental errors.
- Geopolymer materials appear as porous materials, light-weight, fire resistant, and moisture retaining materials with potential sound and thermal insulating properties when comparing the results obtained with those of existing conventional insulating materials.

- Optimal composition can be designed through control of Si/Al molar ratio, alkali content, and crystalline phase content with low thermal conductivity.
- The relative low thermal conductivity confirms geopolymer as potential materials for insulation especially in building construction and refrigeration equipment.

References

1. Bauer TH. A general analytical approach toward the thermal conductivity of porous media. Int J Heat Transf. 1993;36:4181–91.
2. Woodside W, Messmer JM. Thermal conductivity of porous media. J Appl Phys. 1961;32(9):1688–706.
3. Samantray PK, Karthikeyan P, Reddy KS. Estimating effective thermal conductivity of two-phase materials. Int J Heat Mass Transf. 2006;49:4209–19.
4. Côté J, Konard J-M. Assessment of structure effects on the thermal conductivity of two-phase porous geomaterials. Int J Heat Mass Transf. 2009;52:786–804.
5. Zschiegner S, Russ S, Bunde A, Karger J. Pore opening effects and transport diffusion in the Knudsen regime in comparison to self- (or tracer) diffusion. Lett J Explor Front Phys. 2007;78:20001–5.
6. Stark I, Stordeur M, Syrowatka F. Thermal conductivity of thin amorphous alumina films. Thin Solids Films. 1993;226:185–90.
7. Demirboga R, Gul R. The effects of expanded perlite aggregate silica fume and fly ash on the thermal conductivity of lightweight concrete. Cem Concr Res. 2003;33:723–7.
8. Fu X, Chung DDL. Effects of silica fume, latex, methylcellulose, and carbon fibers on the thermal conductivity and specific heat of cement paste. Cem Concr Res. 1997;27:1799–804.
9. Macgree AE. Some thermal characteristics of clays. J Am Ceram Soc. 1927;10(8):561–8.
10. Michot A, Smith DS, Degot S, Gault C. Thermal conductivity and specific heat of kaolinite: evolution with thermal treatment. J Eur Ceram Soc. 2008;28:2639–44.
11. Cheng TW, Chiu JG. Fire-resistant geopolymer produced by granulated blast furnace slag. Miner Eng. 2003;16:205–10.
12. Comerie DC, Kriven WM. Composite cold ceramic geopolymer in a refractory application. Ceram Trans. 2003;153:211–25.
13. Duxson P, Luckey GC, van Deventer JSJ. Thermal conductivity of metakaolin geopolymers used as a first approximation for determining gel interconnectivity. Ind Eng Chem Res. 2006;45:7781–8.
14. Prud'Homme E, Michaud P, Joussein E, Peyratout C, Smith A, Rossignol S. In situ inorganic foams prepared from various clays at low temperature. Appl Clay Sci. 2011;51(1–2):15–22.
15. Prud'homme E, Michaud P, Joussein E, Peyratout C, Smith A, Arri-Clacens S, Clacens JM, Rossignol S. Silica fume as porogent agent in geo-materials at low temperature. J Eur Ceram Soc. 2010;30:1641–8.
16. Pouchon MA, Degueldre C, Tissot P. Determination of the thermal conductivity in zirconia based inert matrix nuclear fuel

by oscillating differential scanning calorimetry and laser flash. Thermochim Acta. 1998;323:109–21.

17. Gilbert B, Mainprice D. Effect of crystal preferred orientations on the thermal diffusivity of quartz polycrystalline aggregates at high temperature. Teconophysics. 2005;465:150–63.

18. Enguehard F. Multiscale modelling of radiation heat transfer through nanoporous superinsulating materials. Int J Thermophys. 2007;28(5):1693–717.

19. Parker WJ, Jenkins RJ, Butler CP, Abbott GL. Flash method of determining thermal diffusivity, heat capacity and thermal conductivity. J Appl Phys. 1961;32:1679–84.

20. Lachi M, Degiovanni A. Determination des diffusivités thermiques des matériaux anisotropes par methode flash bidimensionnelle. J Appl III. 1991;1:2027–46.

21. Degiovanni A, Laurent M. Une nouvelle technique d'identification de la diffusivité thermique pour la methode flash. Rev Phys Appl. 1986;21:229–37.

22. Mojumdar SC, Sain M, Prasad RC, Sun L, Venart JES. Selected thermoanalytical methods and their applications from the medicine to construction, part I. J Therm Anal Calorim. 2007;90(3): 653–62.